Article

Sodium-Selective Fluoroionophore-based Optodes for Seawater Salinity Measurement

Bernhard J Müller, Tanja Rappitsch, Christoph Staudinger, Christian Rüschitz, Sergey M Borisov, and Ingo Klimant

Anal. Chem., **Just Accepted Manuscript** • Publication Date (Web): 06 Jun 2017

Sodium-Selective Fluoroionophore-based Optodes for Seawater Salinity Measurement

Bernhard J. Müller, Tanja Rappitsch, Christoph Staudinger, Christian Rüschitz, Sergey M. Borisov and Ingo Klimant*

Graz University of Technology, Institute of Analytical Chemistry and Food Chemistry, Stremayrgasse 9, 8010 Graz, Austria
E-mail: sergey.borisov@tugraz.at

Keywords

Optical Sensor, Sodium, Salinity, Photoinduced Electron Transfer, Fluoroionophore, Hydrogel, Fluorescence

Abstract

A new fluorescent sensor for Na^+ is presented. The sensor relies on a Na^+ selective fluoroionophore based on a bright red-emitting BODIPY chromophore. The fluorescence of the fluoroionophore is enhanced upon binding of Na^+-ions to the highly selective aza-crown ether receptor due to reduction of the photoinduced electron transfer (PET) quenching.

Solid state sensing materials were prepared by physically embedding the fluoroionophore into water-swellable biocompatible polymer matrices (polyurethane hydrogels), thus enabling continuous measurements of aqueous samples. Despite the simple design, the sensor showed no leaching of the indicator and featured fast and reversible response.

Among different polyurethane hydrogels investigated, the hydrogel D1 featuring the highest water uptake was found to be the most suitable due to the highest dynamics between "off" and "on" states. Due to little or no cross sensitivity to other ions (e.g. Mg^{2+}, Ca^{2+}, K^+) and its insensitivity to potential changes in pH, this sensor is promising for use in clinical diagnostics and for biological and marine applications. Fiber optic sensors based on referenced read-out with a compact phase fluorimeter were prepared. To demonstrate their practical applicability, the sensors were used to determine the salinity in the seawater and brackish water of the Baltic Sea.

Introduction

Optical sensors (Optodes) are promising analytical tools for *in situ* measurements, with several properties making them advantageous to the conventional analytical methods. They are non-invasive, disposable, can be miniaturized easily and when combined with other sensors, they enable multi-analyte measurements.[1] Moreover, they allow imaging of analytes over a certain area or even in small volumes (e.g. cells).[2,3] Optical sensing materials are widely used in various formats such as mini- and microsensors [4,5,6,7], planar sensor foils [8,9] and nanoparticles [10,11].

There is significant interest in development of new optical sensors for a variety of analytes, for instance oxygen, pH, carbon dioxide, reactive oxygen species or ions.[12] Ions play an essential role in all living organisms and natural processes.[13] Sodium is a crucial factor for physiological pathways in the biomedical field. It is the most abundant ion in the extracellular medium (more than 100 mM) and is maintained at a low intracellular concentration, creating an osmotic pressure which is crucial for the transmission of nerve impulses.[14] Determination and visualisation of the transport of ions between the inner and outer compartment of the cell is of high interest for biological research and can be achieved by utilizing fluorescent probes.[15,16,17,18] Optical sensors for cations can be divided into two main groups. The first group relies on use of hydrophobic membrane (poly(vinyl chloride) with plasticizer) containing an analyte selective ionophore and a pH indicator. Selective extraction of the target analyte into the lipophilic membrane triggers a release of an equivalent amount of protons out of the sensing film, thereby changing the pH which can be measured by a lipophilic pH indicator.[19]

In the second group the fluorescent reporter and the receptor are combined in a single molecule (fluroionophore, FI). FIs operate in aqueous media and have been mostly applied as water-soluble probes. Several FI-based probes for Na^+ have been reported [20,21,22,23,24,25,26,27] primarily in the context of intracellular measurements. The sensing mechanism is based on intramolecular quenching via photoinduced electron transfer (PET).[28,29,30] The most popular and commercially available sodium FIs are SBFI (sodium binding benzofuran isophthalate) and SG (sodium green).[14,31] They consist of a diaza-15-crown-5 ether as a receptor coupled to a benzofuran or a fluorescein fluorophore, respectively. However, all of these indicators possess a relatively short excitation wavelength (below 500 nm), leading to high (and variable) levels of background fluorescence from optical components, carrier polymers, and biological samples. Fluorescein is known for its poor photostability. Therefore, new FIs with

longer wavelengths of absorption and emission (> 600 nm) are of particular interest as they allow measurements in highly scattering and absorbing media (e.g. tissues) as well as in autofluorescent media (e.g. biological samples).

Design of FI-based ion sensors is a challenging task since the FI should not only retain its sensitivity upon immobilization but also show no leaching out of the matrix. Thus, the matrix should be hydrophilic enough to ensure sufficient PET efficiency (which is known to decrease in a low polarity environment) but hydrophobic enough to be a good solvent for the non-covalently immobilized amphiphilic FI or contain functionalities for the covalent coupling of a hydrophilic FI. So far, only very few published indicators were immobilized in a polymer matrix, all of them short wavelength FIs.[32,33,34]

In this contribution, we present a novel sensor for Na^+-ions based on hydrogel-immobilized fluoroionophore. We take advantage of the complexation properties of a crown ether receptor that has an appropriate size to selectively bind Na^+-ions. This receptor is linked to a red light emitting BODIPY chromophore which features high brightness and excellent photostability. The aromatic amino group in the receptor acts as efficient fluorescence quencher in the absence of the analyte but the fluorescence is dramatically enhanced upon complexation. Based on the correlation between Na^+ concentration and seawater salinity, we demonstrate applicability of the new optical sensor for oceanographic applications.

Materials and Methods

^1H NMR and ^{13}C spectra were recorded on a 300 MHz instrument from Bruker. MALDI-TOF mass spectra were recorded on a Micromass TofSpec 2E in reflectron mode at an accelerating voltage of +20 kV. Absorption measurements were performed on a Cary 50 UV-Vis spectrophotometer from Varian. Luminescence spectra and absolute quantum yields were measured on a Fluorolog-3 luminescence spectrometer (Horiba). Calibrations were performed by fixing a sensor foil diagonally in a quartz cuvette filled with different buffer solutions. QY of the indicator in solution (THF in presence of 0.3 mM trifluoroacetic acid) and in sensor foils (at 1000 mM NaCl and 0.1 M aqueous HCl) were acquired with an integrating sphere from Horiba. Leaching was investigated by recording the absorption spectra of a foil during continuous pumping a TRIS-buffered (7.4) solution with 500 mM NaCl through a flow-through cell (15 ml/min). Measurements of the referenced sensors were performed with

FirestingO$_2$ and FirestingGO$_2$ phase fluorimeters (www.pyro-science.com) at a modulation frequency of 4 kHz and a LED intensity of 80 %. Optical plastic fibers (1 mm core diameter) were obtained from Ratioplast-Optoelectronics GmbH (www.ratioplast.eu). Polyurethane hydrogels (Hydromed D1, D4 and D7) were purchased from AdvanSource biomaterials (www.advbiomaterials.com). Poly(ethylene terephthalate) support Melinex 505 was obtained from Pütz (www.puetz-folien.com). Hydrochloric acid 37% (HCl), anhydrous sodium sulfate and all other solvents including the deuterated solvents were from VWR (www.vwr.com). Polysulfone (Mn=16000, Mw=35000), 2,3-dichloro-5,6-dicyano-p-benzoquinone (DDQ), trifluoroacetic acid, boron trifluoride etherate ($BF_3{\cdot}O(C_2H_5)_2$), DMF, $POCl_3$ and water-free dichloromethane (DCM) were purchased from Aldrich (www.sigmaaldrich.com). Buffer substances, NaCl, KCl, $CaCl_2$, $MgCl_2$, K_2CO_3, KI, KOH and chloroform (analytical grade) were from Roth (www.carlroth.com). Silica gel (0.04-0.063 mm) was acquired from Acros Organics (www.fishersci.com). Carbon black was obtained from Kremer Pigments (www.kremer-pigmente.com). Monocrystalline diamond powder was purchased from Microdiamant (www.microdiamant.com). Silanized Egyptian blue microparticles (trimethylsilyl form) were prepared according to a literature procedure.[35] All other chemicals were purchased from TCI Europe (www.tcichemicals.com). All chemicals were used as received.

Experimental

5-Chloro-3-phenyl-1,4-dihydroindeno[1,2-b]pyrrole (6)

This synthesis was performed according to the literature procedure.[36]

Triethylene glycol ditosylate (3)

Triethylene glycol (4.50 g, 30.0 mmol, 1 eq) and 4-toluenesulfonyl chloride (11.80 g, 61.8 mmol, 2.1 eq) were dissolved in 100 ml dichloromethane (DCM). The solution was cooled down to 0 °C and portions of KOH (13.60 g, 242.3 mmol, 8.1 eq) were added slowly over a period of 15 min and then allowed to warm up to RT over 4 hours. H_2O (60 ml) was added and the reaction mixture was extracted (DCM) (2x, 30 ml). The organic phase was dried over Na_2SO_4 and the solvent was removed using a rotary evaporator. The crude product was recrystallized from methyl tert-butyl ether (MTBE) to yield a white crystalline product (10.40 g, 75 %). ^{1}H NMR (300 MHz, $CDCl_3$) δ 7.79 (d, J = 8.2 Hz, 4H), 7.34 (d, J = 7.9 Hz, 4H),

4.16 – 4.11 (m, 4H), 3.67 – 3.63 (m, 4H), 3.52 (s, 4H), 2.44 (s, 6H). ^{13}C NMR (76 MHz, $CDCl_3$) δ 145.02, 130.02, 128.13, 70.87, 69.37, 68.93, 21.81.

***N,N*-bis(2-Hydroxylethyl)-2-methoxyaniline (2)**

A mixture of 2-anisidine (**1**) (21.84 g, 0.177 mol, 1 eq), 2-chloroethanol (52.8 g, 0.655 mol, 5 eq), $CaCO_3$ (17.75 g, 0.177 mol, 1 eq) and KI (2.27 g, 0,013 mol, 0.07 eq) was stirred in 300 ml H_2O at 90 °C until TLC indicated full conversion (eluent: cyclohexane (CH) + ethyl acetate (EA), 1+2). The reaction mixture was filtered, the filtrate extracted with DCM and the organic phase dried over Na_2SO_4 before removing the solvent in vacuo. The crude product was purified using column chromatography (eluent DCM to EA and then EA + MeOH (90+10)) to yield the product as brown oil (15.36 g, 40.9 %). ^{1}H NMR (300 MHz, CD_2Cl_2) δ 7.25 – 7.08 (m, 2H), 7.02 – 6.90 (m, 2H), 3.85 (s, 3H), 3.50 – 3.44 (m, 4H), 3.20 – 3.15 (m, 4H), 3.10 (bs, 2H). ^{13}C NMR (76 MHz, CD_2Cl_2) δ 155.84, 138.90, 125.99, 125.24, 121.78, 112.08, 60.10, 57.60, 55.87.

2-Methoxyphenylaza-15-crown-5 (4)

NaH (3.243 g of 60% NaH suspension in mineral oil, 81.0 mmol, 2.5 eq) was added slowly to anhydrous tetrahydrofuran (THF) (150 ml) under an argon counterflow. The mixture was heated to reflux and a solution of N,N-bis(2-hydroxylethyl)-2-methoxyaniline (**2)** (6.719 g, 31.8 mmol, 1 eq) and triethylene glycol ditosylate (**3**) (14.66 g, 31.8 mmol, 1 eq) dissolved in 100 ml anhydrous THF was added dropwise over a period of 30 min and continued refluxing for 18 hours. After cooling down, the suspension was filtered and the solvent was removed under reduced pressure. The residue was dissolved in 20 ml MeOH, heated to reflux and $NaClO_4 \cdot H_2O$ (4.84 g, 34.45 mmol, 1.08 eq) dissolved in 10 ml MeOH was added. After 30 min, 20 ml EA was added and the solution was concentrated to a volume of 10 ml on the rotary evaporator. This suspension was refluxed and EA was added until a total volume of 450 ml. The clear solution was then put in the fridge for 18 hours. The obtained white crystals were filtered, dried in an oven and then dissolved in 10 ml DCM and extracted with H_2O (3x 10 ml) to obtain the free crown (2.80 g, 27 %). ^{1}H NMR (300 MHz, $CDCl_3$) δ 7.12 (dd, J = 7.5, 2.0 Hz, 1H), 6.98 – 6.81 (m, 3H), 3.83 (s, 3H), 3.73 – 3.64 (m, 16H), 3.52 – 3.44 (m, 4H). ^{13}C NMR (76 MHz, $CDCl_3$) δ 152.78, 140.08, 122.12, 120.84, 120.74, 111.77, 70.97, 70.60, 70.37, 70.18, 55.40, 53.00. MS (MALDI-TOF): m/z $[MNa]^+$ 348.1787 calcd, 348.1895 found.

4-Formyl-2-methoxyphenylaza-15-crown-5 (5)

2-Methoxyphenylaza-15-crown-5 (**4**) (2.51 g, 7.7 mmol, 1 eq) was dissolved in 4 ml DMF in a Schlenk flask, cooled down to -8 °C and $POCl_3$ (1.68 g, 16.1 mmol, 2.1 eq) was added slowly so that the temperature did not raise over 0 °C. Afterwards, the reaction mixture was allowed to warm up to RT and was stirred for 20 hours and then heated to 60 °C for 2 hours. Aldehyde formation could be seen by TLC (DCM + MeOH, 75 + 5) and staining of the TLC with a solution containing dinitrophenylhydrazine (DNP). The solution was cooled down to RT, poured slowly over ice and neutralized with K_2CO_3 to pH 7. The reaction mixture was extracted with DCM (3x, 30 ml), the solvent was removed and the product purified by column chromatography (gradually from DCM to DCM + MeOH, 100+5) to yield the product as brown oil (1.12 g, 41 %). ^{1}H NMR (300 MHz, CD_2Cl_2) δ 9.73 (s, 1H), 7.38 – 7.28 (m, 2H), 6.98 (d, J = 8.3 Hz, 1H), 3.84 (s, 3H), 3.72 – 3.64 (m, 4H), 3.62 – 3.55 (m, 15H). ^{13}C NMR (76 MHz, CD_2Cl_2) δ 190.49, 151.36, 146.49, 129.04, 126.71, 116.80, 110.42, 71.3, 70.74, 70.56, 70.32, 55.91, 54.05. MS (MALDI-TOF): m/z $[MH]^+$ 354.1917 calcd, 354.1599 found.

BODIPY Fluoroionophore (Na-FI)

4-Formyl-2-methoxyphenylaza-15-crown-5 (**5**) (1.10 g, 3.11 mmol, 1 eq) and 5-chloro-3-phenyl-1,4-dihydroindeno[1,2-b]pyrrole (**6**) (1.69 g, 6.38 mmol, 2.05 eq) were dissolved in 5 mL of anhydrous DCM and 1 drop of trifluoroacetic acid was added. The mixture was shielded from light and stirred at RT for 48 hours and 2,3-dichloro-5,6-dicyano-1,4-benzoquinone (DDQ) was added (0.741 g, 3.26 mmol, 1.04 eq), changing the colour of the reaction mixture to dark blue. After stirring for another 15 min, N,N-diisopropylethylamine (DIPEA) (4.07 g, 31.4 mmol, 10 eq) and $BF_3{\cdot}O(C_2H_5)_2$ (6.9 g, 48.6 mmol, 15 eq) were added under argon counterflow. After 15 minutes stirring, the mixture was extracted with H_2O, the organic phase was dried over Na_2SO_4 and the solvent removed in vacuo. Purification was performed by column chromatography (2x, eluent DCM gradually to DCM + MeOH, 100+5) yielding the product as purple crystals (211 mg, 7.4 %). UV-VIS (DCM): λmax = 538 nm, ε = 130,000 $M^{-1}cm^{-1}$. ^{1}H NMR (300 MHz, CD_2Cl_2) δ 8.30 (d, J = 8.4 Hz, 2H), 7.54 – 7.45 (m, 4H), 7.05 – 6.83 (m, 10H), 6.66 – 6.58 (m, 2H), 6.39 – 6.31 (m, 1H), 3.82 – 3.45 (m, 27H). MS (MALDI-TOF): m/z $[MNa]^+$ 934.2782 calcd, 934.2747 found.

Planar sensor films

Hydrogel polymers (Hydromed D1, D4 or D7) were dissolved in THF to yield a solution of 10 wt.%. An appropriate amount of the indicator was dissolved in the hydrogel solution. The sensor films were prepared by knife coating of these "sensor cocktails" onto dust-free polyester foils (25 µm wet film thickness). The sensor foils were allowed to dry for several hours at RT. Dye concentrations for calibrations and QY determination were 0.2 wt.% and for leaching experiment 1 wt.% in respect to the polymer.

Fiber-optic sensor for ratiometric DLR readout

The "cocktail" for the reference layer was prepared by dispersing 12 mg Egyptian blue and 100 mg polysulfon in 888 mg $CHCl_3$. This "cocktail" was knife coated onto dust-free polyester foils (25 µm wet film thickness) and allowed to dry in the oven at 60 °C for 2 hours. For the first sensing layer 0.5 mg **Na-FI**, 100 mg diamond powder and 100 mg hydrogel D1 were dispersed/dissolved in 566 mg THF. This "cocktail" was knife coated onto the back-side of the polyester support and allowed to dry for 2 hours at RT (75 µm wet film thickness). The cover layer was prepared by dissolving/dispersing 0.5 mg **Na-FI**, 100 mg carbon black and 100 mg hydrogel D1 in 566 mg THF (15 wt.% in respect to the polymer). This "cocktail" is knife coated onto the first sensor layer (25 µm wet film thickness) and allowed to dry for 2 hours at RT. A sensor spot was then either stamped out (2 mm diameter) and fixed with a metal cap on a 1 m PMMA fiber or stamped out (5 mm diameter) and glued on a plastic screw cap.

Results and Discussion

Synthesis and Photophysical Properties of the New Fluoroionophore

The synthesis of the fluoroionophore is based on a convenient approach previously demonstrated for K^+ FIs.[36] The sensitivity towards the analyte is controlled by the aromatic crown-ether receptor unit, whereas the spectral properties are determined by the BODIPY chromophore. Condensation of the pyrrole and the aromatic aldehyde, subsequent oxidation using DDQ and complexation with BF_3-etherate yields the new fluoroionophore (**Na-FI**) in a simple one-pot reaction (**Figure 1**).

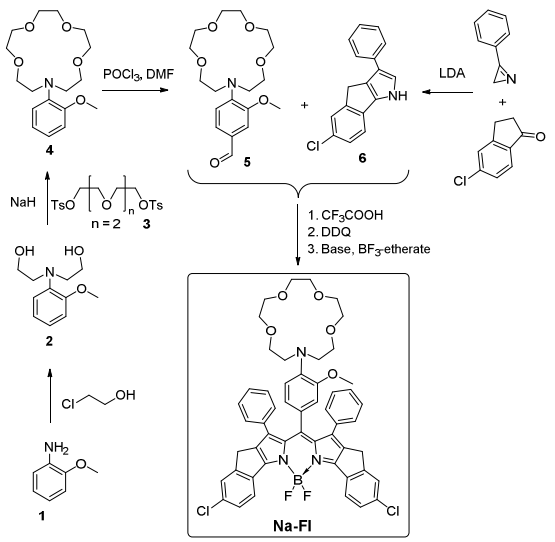

Figure 1. Synthesis of the Na^+ fluoroionophore (**Na-FI**).

As a receptor, we chose a methoxy-substituted N-phenyl-aza-crown ether due to its optimal binding constant towards Na^+ ions.[37] This crown ether was already used as the recognition unit in Na^+ FIs based on naphthalimide [34] and triazole–coumarin derivates.[33] Based on our experience with K^+ FIs, a rigid tetraaryl-BODIPY dye was selected since the rigidification and planarization of the chromophore results in a bathochromic shift of absorption and emission and ensures excellent fluorescence brightness.[36] Indeed, the FI shows efficient absorption and emission in the red/NIR region of the electromagnetic spectrum (**Figure 2**). The absorption and emission bands are very sharp which is typical for BODIPY dyes.[25] It also features excellent luminescence brightness due to high molar absorption coefficient (130,000 $M^{-1}cm^{-1}$) and a quantum yield of 69 % in the "on" state (fully protonated in THF using trifluoroacetic acid). The introduction of chlorine favourably affects the PET efficiency, as the electron withdrawing character enhances the reduction potential of the fluoroionophore in the excited state.[36] Therefore, the fluorescence is almost completely "switched off" when no analyte is present.

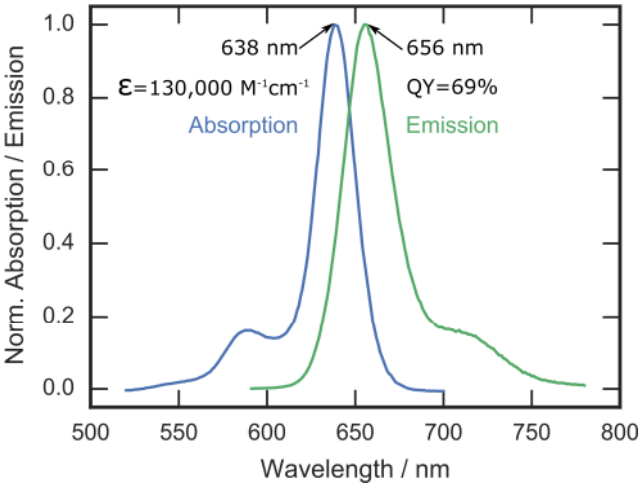

Figure 2. Normalized absorption and emission spectra of the fluoroionophore dissolved in dichloromethane. Molar absorption coefficient was determined in dichloromethane and the quantum yield in tetrahydrofuran with 0.3 mM trifluoroacetic acid to ensure full protonation of the crown ether.

Solid State Sensing Materials

To enable continuous measurement, it is necessary to immobilize the FI into a polymer matrix. Although covalent coupling represents the most efficient strategy to eliminate indicator migration and leaching, several additional synthetic steps would be necessary to introduce the required functionalities which in turn may negatively affect the photophysical properties of the FI. Therefore, we preferred non-covalent immobilisation.

This can be achieved by simply dissolving the indicator dye and the polymer in an organic solvent and knife-coating of the solution onto a transparent and inert poly(ethylene-terephthalate) foil, which acts as sensor support. The polymer matrix acts as a solvent for the indicator dye and therefore cannot be too hydrophobic (due to poor PET in hydrophobic environment) or too hydrophilic, as the FI can either leach out of the matrix or aggregate. Therefore, we chose commercially available water swellable hydrogels (known under the name Hydromed D1, D4 and D7) which are ether-based polyurethanes with hydrophobic and hydrophilic blocks. Depending on the ratio of the blocks, they show different swelling (water uptake) behaviour: swollen hydrogels D1, D4 and D7 contain 70 %, 50 % and 30 % water, respectively.[38] Importantly, no leaching or aggregation of the immobilized FI was observed upon continuous rinsing of the sensor foil with a 500 mM NaCl solution for several hours even in case of the most hydrophilic hydrogel D1 and high dye concentration (1 wt.%). (**Figure S1** and **S2**, Supporting Information).

Influence of the Polymer Matrix

As expected, the immobilized FIs show low fluorescence intensity in the absence of the analyte (**Figure 3**). The fluorescence intensity of the indicator dye is enhanced in the presence of Na^+ due to the decrease of the PET effect. The sensing behaviour of the FI is strongly influenced by the hydrophilicity of the hydrogel used. The fluorescence enhancement factor is the highest (12-fold at 1000 mM Na^+) in more hydrophilic hydrogel D1. In case of the most hydrophobic hydrogel D7, fluorescence is enhanced only 4-fold in the same conditions. Hydrogel D4 occupies intermediate position (**Table 1**, **Figure S3,** Supporting Information).

In the absence of Na^+, fluorescence quantum yields are very similar for all the hydrogels (**Table 1**). However, at high Na^+ concentration (1000 mM), the quantum yields are very different: D1 > D4 > D7. The same trend is observed for fluorescence enhancement in acidic media. pH calibration curves show, that the FI is completely "switched on" only in case of hydrogel D1 and D4 (QY of 86 % and 84 % respectively in 0.1 M HCl) (**Figure S4**, Supporting Information). In case of D7, a QY of 50 % was determined in 0.1 M HCl. However, it was not possible to fully protonate the FI with even highly concentrated HCl solutions (**Figure S4**, Supporting Information). The dye appears to be located in more hydrophobic domains, which are not fully accessible to Na^+-ions or protons. This difference in analyte accessibility is indicated by the decrease of the apparent pK_a value and decrease of QYs in 1000 mM Na^+ with increase in the hydrogel hydrophobicity (**Table 1**). Among the investigated hydrogels, D1 has the highest degree of swelling and therefore best accessibility of the FI to Na^+. Even though the QY in hydrogel D1 in presence of 1000 mM Na^+ is 23 %, the overall brightness is very good considering high molar absorption coefficients. High brightness allows reduction of the thickness of the sensing layer which is beneficial for the development of sensors with fast response time. An LOD of 1.3 mM Na^+ was calculated when using hydrogel D1 (3 x standard deviation of the blank). Due to the best performance, the sensing material based on hydrogel D1 was chosen for further experiments.

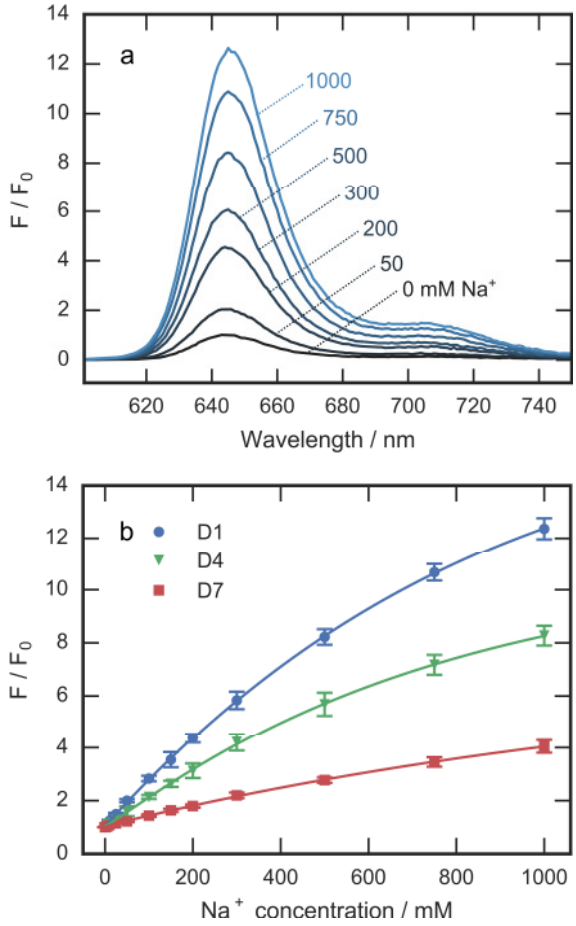

Figure 3.a: Exemplar normalized emission spectra of **Na-FI** in hydrogel D1 at different Na^+ concentrations (20 mM TRIS buffer pH 7.4) **b:** F/F_0 calibration curves for the indicator immobilized in hydrogel D1, D4 and D7. The values of F and F_0 were taken at $\lambda = 645$ nm.

Table 1. Fluorescence intensity ratios F/F_0 at 645 nm and fluorescence quantum yields for **Na-FI** in different hydrogel matrices.

	F/F_0 at 1000 mM NaCl	QY at 0 mM NaCl	QY at 1000 mM NaCl	QY at 0.1 M HCl	Apparent pK_a value
Hydrogel D1	12.4	0.01	0.23	0.86	3.03
Hydrogel D4	8.3	0.01	0.16	0.84	2.60
Hydrogel D7	4.0	0.02	0.09	0.50	1.46*

*pK_a was estimated assuming a QY of 0.85 in the fully protonated state to enable a sigmoidal fit.

Cross-Sensitivity of the Sensing Material to Cations and Protons

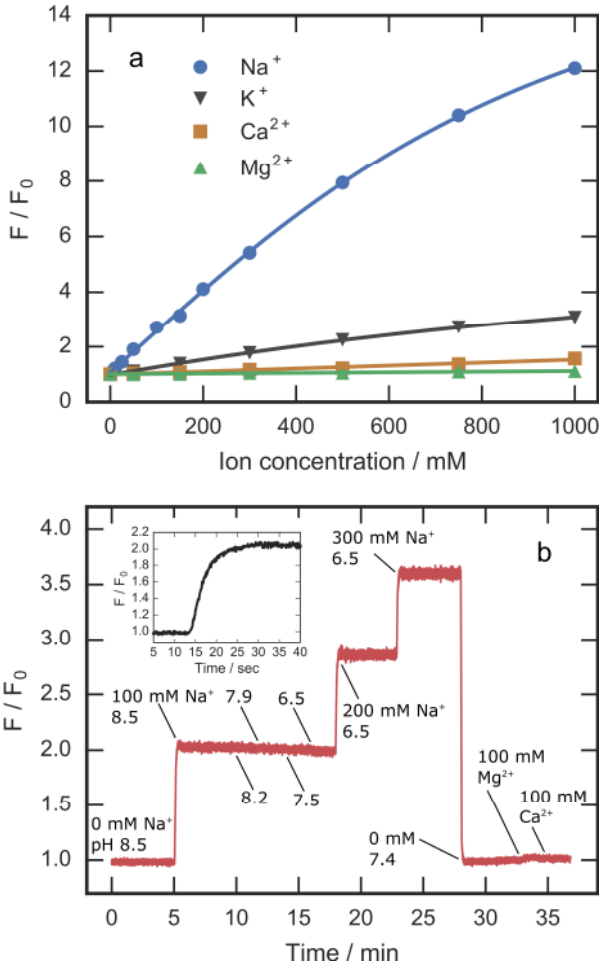

Figure 4.a: Cross-sensitivity of **Na-FI/**D1 to common cations at pH 7.4 (20 mM TRIS buffer). **b**: Fluorescence response detected in the kinetic mode of the fluorimeter. A foil of Na-FI in hydrogel D1 was fixed in a flow-cell and solutions with different Na^+, Mg^{2+}, Ca^{2+} concentrations or pH values were pumped through it. The insert shows a zoom of the response from 0 mM to 100 mM NaCl (t_{90} < 20 sec).

The selectivity of the indicator dye is mostly determined by the size of the recognition unit (crown ether). The cross-talk to cations depends on the size and charge of the ions. The aza-15-crown-5 used in this study is well known for complexing Na^+ and shows good selectivity against other alkali ions. **Figure 4a** shows the selectivity of the FI/ D1sensor. Some cross-talk to K^+ is visible at very high concentrations. However, this interference is not problematic for envisaged applications as very low K^+ is present (e.g. ~ 5 mM in blood and 10 mM in seawater) whereas the concentration of Na^+ is much higher (~150 mM and 500 mM, respectively). In fact, addition of 5 or 10 mM KCl to a solution of 150 mM NaCl does not result in a statistically significant increase of the fluorescence intensity. Addition of as much as 150 mM K^+ shows some enhancement of the signal that would correspond to an increase in

Na^+ concentration from 150 to ~160 mM. Additionally, the ionic strength of the solution is doubled in this test which may also contribute to the observed changes.

Notably, virtually no cross-talk to Ca^{2+} and Mg^{2+} is observed (**Figure 4**). Interestingly, BODIPYs with aza-15-crown-5 without side arms were reported to have rather high cross sensitivity to Ca^{2+} and Mg^{2+}.[39,40,41] Therefore, the side arm of the receptor is likely to be necessary for elimination of this cross sensitivity.

Inertness to pH changes is of major importance for applications of optical ion sensors. Aza-crown ethers based on aromatic amines are advantageous to those containing aliphatic amines due to lower pK_a value (~ 5), which further decreases upon immobilization in the hydrogels (**Table 1**, **Figure S4** Supporting Information) which enables measurements in the physiological pH range without any influence from pH. Indeed, no cross-sensitivity to pH in the range 6.5-8.5 is observed (**Figure 4b**). As can be seen, the response to Na^+ is fully reversible without hysteresis or drift. The dynamic response of about 2.5 µm-thick sensing foil was very fast (t_{90} < 20 seconds).

Miniaturized Referenced Na^+ Optode

All measurements discussed above are intensity based. Fluorescence intensity is affected by many parameters which makes it unsuitable for practical applications. To overcome this limitation dual lifetime referencing (DLR) ratiometric scheme was applied.[42] This method requires a phosphorescent reference dye featuring a long decay time, spectral properties similar to those of the indicator and inertness towards the analyte and other substances. The DLR scheme can be applied both in frequency and in time domain.[42] In the case of the former, the overall phase shift measured by a phase-fluorimeter is determined only by the ratio of the amplitudes of the FI (A_{ind}) and the reference material (A_{ref}) (**Eq. 1**). For instance, if the fluorescence intensity of the indicator is low, mostly the luminescence intensity of the reference material can be detected, and a low cotangent of the overall phase shift (ϕ) is measured. As a reference material, we utilized Egyptian blue, an inorganic phosphor excitable in the green-red part of the electromagnetic spectrum and emitting in the NIR. A good quantum yield of 10 %,[43] a luminescence lifetime of ~107 µs and its high photostability make it an almost ideal reference material for DLR.[35]

$$\frac{A_{ind}}{A_{ref}} = cot\phi \cdot cot\varphi_{ref} - cot\phi_{ref} \quad \text{(Eq. 1)}$$

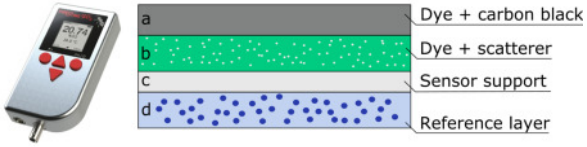

Figure 5. Miniaturized phase fluorimeter FirestingGO_2 from Pyro Science and the cross-section of the sensor for referenced read-out using a phase fluorimeter. **a**: Hydrogel D1 with immobilized indicator dye and carbon black for optical isolation. **b**: Hydrogel D1 with immobilized indicator dye and diamond powder for enhancing signal by light scattering. **c**: sensor support. **d**: Egyptian blue microparticles immobilized in polysulfone.

The referenced sensor consists of three layers coated onto a transparent polyester support (**Figure 5**). Silanized Egyptian blue particles were immobilized in polysulfone (**d**) and coated on the support (**c**). To prevent potential interaction between the reference layer and the sensing layer, we chose to coat the latter on the opposite side, in order to have the polyester foil as a barrier. The other side of the support foil has a layer of hydrogel D1 incorporating the indicator dye and diamond powder for signal enhancement caused by light scattering (**b**). A further hydrogel D1 layer consisting of **Na-FI** and carbon black was used as the final layer (**a**). Carbon black acts as optical isolation in order to prevent interference from ambient light. The dye was added in the same concentration as in layer **b** in order to prevent migration from one layer to the other, thus changing the signal intensities. As both "cocktails" are dissolved in THF, applying the second layer yield to some mixing of the layers. However, as only one type of polymer and the same amount of indicator dye is used in both, this mixing of layers will not cause any disturbing effects. Notably, diamond powder and carbon black are not necessary in order to obtain a referenced sensor, but they improve the sensors performance by elimination of potential interferences caused by background fluorescence and ambient light (which may saturate the photodetector). A sensor spot was stamped out from this material and was mounted either directly onto PMMA fibers using a metal cap, or glued on a plastic screw-cap which could be fixed directly onto the read-out device. A commercially available phase-fluorimeter (FirestingGO_2 from Pyro Science) was used for measurement of the phase shift (**Figure 5**).

Application of Na^+ Optode for Measurement of Seawater Salinity

The salinity of water is an important measure of water quality. The survival of different species of animal and plant life depends on the salinity range within their habitat. The most

abundant cations in seawater are Na^+, Mg^{2+}, Ca^{2+} and K^+, while Cl^-, SO_4^{2-}, Br^- and HCO_3^- are the predominant anions (**Table 2**).[44] The sum of masses of these ionic species is referred to as salinity; it is expressed as practical salinity unit (PSU) which is the mass fraction of salts in water (grams salt per kilogram solution).[45,46,47] The average practical salinity in the open ocean is 35, and typically varies between 33 and 37 PSU, while much lower salinities are found in brackish waters where the seawater is diluted by a high quantity of freshwater (between 0-30 PSU).[44,48] Since the only change occurring to seawater is a change in the entire concentration of dissolved ions (e.g. dilution with water), the ratio of the different ion concentrations is not affected. Consequently, the composition stays the same, enabling the determination of salinity by simply measuring one component of the seawater.[49]

Seawater salinity is typically measured with a conductivity sensor. An optical sensor for determination of salinity via measurement of Cl^- concentration has been reported.[49] Here we propose an alternative method based on quantification of Na^+ concentration.

The dynamic range of the new sensing material based on **Na-FI/**D1 matches very well the concentration of Na^+ present in seawater. As discussed above, the minor cross-sensitivity of the sensor to K^+ is not critical for seawater measurement since the concentration of K^+ is too low to be detected by the sensor (**Table 2**). Advantageously, comparably high concentrations of Mg^{2+} occurring in seawater do not trigger any fluorescence response.

Table 2. Summary of mean composition of seawater with salinity 35 at 25 °C.[49]

Cations	g/kg	mM	Anions	g/kg	mM
Na^+	**10.77**	**479**	Cl^-	19.37	559
Mg^{2+}	1.30	54.4	SO_4^{2-}	2.71	28.9
Ca^{2+}	0.409	10.5	CO_3^{2-}	0.0026	2.33
K^+	0.388	10.4	Br^-	0.065	0.86
Sr^{2+}	0.010	0.09	F^-	0.0013	0.075

Determination of temperature cross-talk of the optical sensor is essential for *in situ* monitoring of seawater salinity. A high dependency towards temperature was observed within the relevant concentrations (**Figure 6**). This can be attributed to the influence of temperature on

the stability constant of the crown ether-Na^+ complex. At higher temperatures, the complexation of the analyte is less favourable, and therefore less fluorescence emission is observed (lower cotangent ϕ). In addition to the complexation equilibrium, Egyptian blue contributes to the temperature dependency, as the emission intensity and lifetime decrease with increasing temperature.[35] This dependency can be compensated for with simultaneous temperature measurements and with the introduction of the temperature coefficient into the calibration equation (**Eq. 2**). A is the upper limit of the fit (PSU 45), B the minimum value (PSU 0) and k describes the increment of the fit. A_T, B_T and k_T are linear temperature coefficients for the three parameters and T represents temperature.

$$\cot(d\phi) = (A + A_T \cdot (T - 20)) \cdot (1 - e^{(-(k + k_T \cdot (T-20)) \cdot Na)}) + (B + B_T \cdot (T - 20)) \quad \text{(Eq. 2)}$$

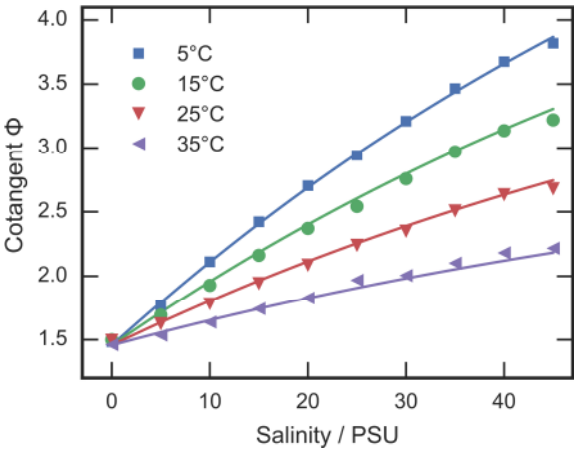

Figure 6. Temperature-dependent calibration of the salinity optode based on Na^+ transduction performed with a phase fluorimeter and an optical plastic fiber with a sensor spot attached to the distal end of the fiber.

Measurement of Salinity in the Baltic Sea

The applicability of this novel sensor was demonstrated in *in situ* measurements of the salinity in the Baltic Sea. We used two different read-out devices for three different application areas. A commercially available handheld phase fluorimeter (FirestingGO_2, Pyro Science) incorporating a PMMA fibre with the sensing material coated on the tip was used for quick *in situ* salinity measurements. Additionally, we conducted salinity profiling measurements up to a depth of 25 m and surface salinity measurements. For this purpose, the stand alone phase fluorimeter was embedded into a polyoxymethylene (POM) pressure housing to enable autonomous long term measurements. The module is also equipped with an internal

temperature sensor, and the Na^+ sensitive material is mounted on the optical feedthrough with a screw-cap system.

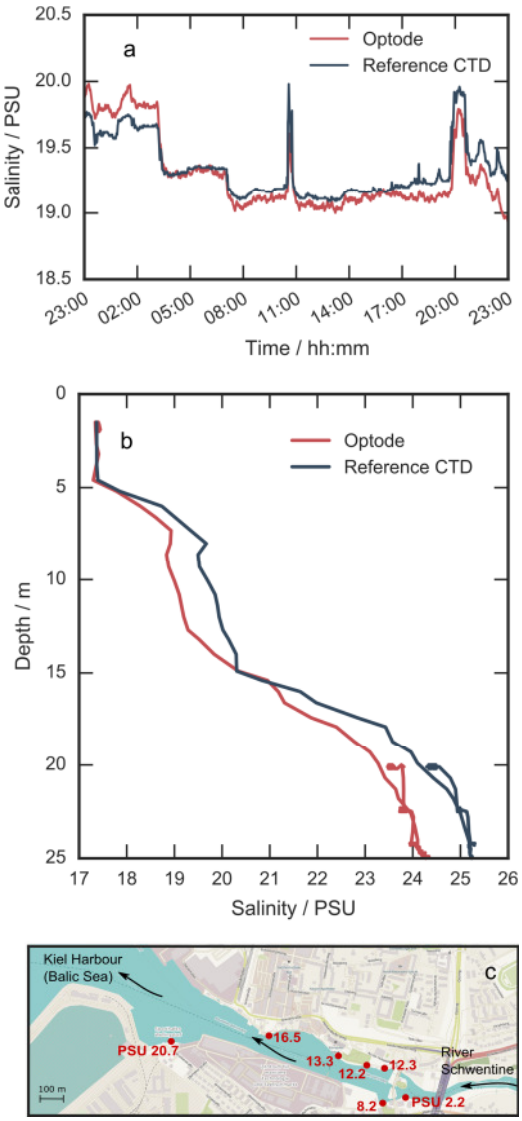

Figure 7. Measured salinity in the Baltic Sea compared to reference conductivity measurements from the CTD rosette. **a**: Measurement performed in surface water for one day (Kiel, 54.3301°N , 10.1498°E). **b**: Profiling measurement with a speed of 0.15 m/s and stops of 10 min at 24, 22 and 20 m acquired at Boknis Eck (54.5° N, 10.0° E). **c:** Measurement points and salinity values determined with the sensor material and a handheld phase fluorimeter as the read-out device.

Figure 7a shows the 24 h measurement of salinity in surface water. The temperature varied between 18.5 °C and 20 °C during the measurement time. The sensor was calibrated at room temperature before deployment with appropriate salinity solutions containing Na^+ ranging from 0 to 1000 mM. Our data is in good agreement with the reference data obtained via conductivity measurements (CTD). The sensor responds sufficiently fast to detect small

changes in salinity. **Figure 7b** shows profiling measurements up to 25 m depth. Contrary to the surface measurement, the first measured point of the CTD at the surface was used as a reference calibration point for the optode, as it showed an offset of around 4 PSU. The trend of salinity measured by the sensor is in good agreement with the reference measurement. However, there is a disparity beyond a depth of 5 m. A possible explanation for this is the reduction in response time at lower temperatures. A combination of the high speed of profiling (0.15 m/s) and the change in temperature at greater depths (from 19.4 °C at 5 m to 11.3 °C at 25 m) could cause this variation to the reference. Preparing thinner sensor foils featuring faster response may overcome this issue.

Several point measurements along the mouth of river Schwentine (Kiel) have also been performed (**Figure 7c**). The lowest salinity (2.2 PSU) was measured in the river before a bridge. There was a gradient in the altitude of about 1-1.5 m with water flowing in the direction of the sea, which prevents movement of the salt water upwards to the river. As the river gets wider, measurements at locations closer to the harbour indicated an increase in the salinity. The last point of measurement is virtually a fjord and the widest location of all measurements, with the highest salinity of 20.7 PSU. This is in good agreement with commonly measured salinity values in the harbour. Using this optode, it was possible to perform *in situ* salinity measurements along a river in minimal time, effort and equipment.

Conclusions

A highly selective optical sensor material for the measurement of Na^+-ions in aqueous media was presented. The new fluoroionophore is based on a aza-crown ether receptor unit coupled to a BODIPY chromophore which shows emission in the red region of the spectrum and good fluorescence brightness. By incorporating this fluoroionophore into a polymer matrix a robust and fast responding sensor is obtained. Among different polyurethane hydrogels tested as matrices the most hydrophilic D1 hydrogel proved to be the most suitable. The material showed the highest dynamics between the “off” and “on” state and the highest fluorescence quantum yield in the “on” state. The sensor displays high selectivity over other competing ions (e.g. Mg^{2+}, Ca^{2+}, K^+) and is not affected by pH changes in the relevant range. As all chemosensors, the sensor shows cross-talk to temperature which can be easily compensated for.

A referenced sensing material has also been prepared to enable measurements with a commercially available compact phase fluorimeter. These sensors were used to determine the salinity of seawater and brackish water in the Baltic Sea, and show good correlation with reference measurements. They demonstrate the potential of optical technology for measuring of this very important parameter. It should be emphasized that the new indicator and sensing materials can also be used for a variety of other applications, such as clinical diagnostics or biological imaging.

Acknowledgment

We thank Prof. Eric Achterberg and the GEOMAR team for their assistance in field measurements. Financial support from the European Union FP7 Projects SenseOcean (Grant Agreement Number 614141) and SCHeMA (Grant Agreement Number 614002) is gratefully acknowledged.

Associated content

Supporting Information

The Supporting Information is available free of charge on the ACS Publications website at DOI:

Leaching experiments, additional emission spectra, MS spectra.

Author Information

Corresponding Author

*E-mail: sergey.borisov@tugraz.at

ORCID

Sergey M. Borisov: 0000-0001-9318-8273

References

(1) McDonagh, C.; Burke, C. S.; MacCraith, B. D. *Chem. Rev.* **2008**, *108* (2), 400–22.
(2) Schäferling, M. *Angew. Chem. Int. Ed.* **2012**, *51* (15), 3532–3554.
(3) Glud, R. N.; Ramsing, N. B.; Gundersen, J. K.; Klimant, I. *Oceanogr. Lit. Rev.* **1997**, *3* (44), 191.
(4) Rosenzweig, Z.; Kopelman, R. *Anal. Chem.* **1995**, *67* (15), 2650–2654.
(5) Song, A.; Parus, S.; Kopelman, R. *Anal. Chem.* **1997**, *69* (5), 863–867.
(6) Kosch, U.; Klimant, I.; Wolfbeis, O. S. *Fresenius J. Anal. Chem.* **1999**, *364* (1–2), 48–53.
(7) Kühl, M. *Methods Enzymol.* **2005**, *397*, 166–199.
(8) Koren, K.; Kühl, M. *Sens. Actuators B Chem.* **2015**, *210*, 124–128.
(9) Holst, G.; Grunwald, B. *Sens. Actuators B Chem.* **2001**, *74* (1–3), 78–90.
(10) Koren, K.; Jakobsen, S. L.; Kühl, M. *Sens. Actuators B Chem.* **2016**, *237*, 1095–1101.
(11) Borisov, S. M.; Klimant, I. *The Analyst* **2008**, *133* (10), 1302–1307.
(12) Wolfbeis, O. S. *J. Mater. Chem.* **2005**, *15* (27–28), 2657.
(13) Li, J.; Yim, D.; Jang, W.-D.; Yoon, J. *Chem. Soc. Rev.* **2016**.
(14) Minta, A.; Tsien, R. Y. *J. Biol. Chem.* **1989**, *264* (32), 19449–19457.
(15) Kong, X.; Su, F.; Zhang, L.; Yaron, J.; Lee, F.; Shi, Z.; Tian, Y.; Meldrum, D. R. *Angew. Chem. Int. Ed.* **2015**, *54* (41), 12053–12057.
(16) Zhou, X.; Su, F.; Gao, W.; Tian, Y.; Youngbull, C.; Johnson, R. H.; Meldrum, D. R. *Biomaterials* **2011**, *32* (33), 8574–8583.
(17) Hirata, T.; Terai, T.; Yamamura, H.; Shimonishi, M.; Komatsu, T.; Hanaoka, K.; Ueno, T.; Imaizumi, Y.; Nagano, T.; Urano, Y. *Anal. Chem.* **2016**, *88* (5), 2693–2700.
(18) Matsui, A.; Umezawa, K.; Shindo, Y.; Fujii, T.; Citterio, D.; Oka, K.; Suzuki, K. *Chem. Commun.* **2011**, *47* (37), 10407–10409.
(19) Mistlberger, G.; Gaston, C. A.; Bakker, E. *Annu. Rev. Anal. Chem.* **2014**, *7* (1), 483–512.
(20) Kim, M. K.; Lim, C. S.; Hong, J. T.; Han, J. H.; Jang, H.-Y.; Kim, H. M.; Cho, B. R. *Angew. Chem. Int. Ed.* **2010**, *49* (2), 364–367.
(21) Silva, A. P. de; Gunaratne, H. Q. N.; Gunnlaugsson, T.; Nieuwenhuizen, M. *Chem. Commun.* **1996**, No. 16, 1967–1968.
(22) Gunnlaugsson, T.; Nieuwenhuyzen, M.; Richard, L.; Thoss, V. *J. Chem. Soc. Perkin Trans. 2* **2002**, *0* (1), 141–150.
(23) Sarkar, A. R.; Heo, C. H.; Park, M. Y.; Lee, H. W.; Kim, H. M. *Chem. Commun.* **2014**, *50* (11), 1309–1312.
(24) Callan, J. F.; de Silva, A. P.; Magri, D. C. *Tetrahedron* **2005**, *61* (36), 8551–8588.
(25) Boens, N.; Leen, V.; Dehaen, W. *Chem Soc Rev* **2012**, *41* (3), 1130–1172.
(26) Martin, V. V.; Rothe, A.; Diwu, Z.; Gee, K. R. *Bioorg. Med. Chem. Lett.* **2004**, *14* (21), 5313–5316.
(27) Meier, S. D.; Kovalchuk, Y.; Rose, C. R. *J. Neurosci. Methods* **2006**, *155* (2), 251–259.
(28) Silva, A. P. de; Moody, T. S.; Wright, G. D. *Analyst* **2009**, *134* (12), 2385–2393.
(29) Valeur, B.; Leray, I. *Coord. Chem. Rev.* **2000**, *205* (1), 3–40.
(30) De Silva, A. P.; Gunaratne, H. N.; Gunnlaugsson, T.; Huxley, A. J.; McCoy, C. P.; Rademacher, J. T.; Rice, T. E. *Chem. Rev.* **1997**, *97* (5), 1515–1566.
(31) Kuhn, M. A.; Haugland, R. P. Fluorescent ion-selective diaryldiaza crown ether conjugates. US5405975 A, April 11, 1995.
(32) Buchholz, F.; Buschmann, N.; Cammann, K. *Sens. Actuators B Chem.* **1992**, *9* (1), 41–47.

(33) Schwarze, T.; Müller, H.; Ast, S.; Steinbrück, D.; Eidner, S.; Geißler, F.; Kumke, M. U.; Holdt, H.-J. *Chem. Commun.* **2014**, *50* (91), 14167–14170.
(34) He, H.; Mortellaro, M. A.; Leiner, M. J. P.; Young, S. T.; Fraatz, R. J.; Tusa, J. K. *Anal. Chem.* **2003**, *75* (3), 549–555.
(35) Borisov, S. M.; Würth, C.; Resch-Genger, U.; Klimant, I. *Anal. Chem.* **2013**, *85* (19), 9371–9377.
(36) Müller, B. J.; Borisov, S. M.; Klimant, I. *Adv. Funct. Mater.* **2016**, *26* (42), 7697–7707.
(37) Schultz, R. A.; White, B. D.; Dishong, D. M.; Arnold, K. A.; Gokel, G. W. *J. Am. Chem. Soc.* **1985**, *107* (23), 6659–6668.
(38) HydroMed Products http://www.advbiomaterials.com/products/hydrophilic/hydromed.html (accessed Nov 23, 2016).
(39) Rurack, K.; Sczepan, M.; Spieles, M.; Resch-Genger, U.; Rettig, W. *Chem. Phys. Lett.* **2000**, *320* (1–2), 87–94.
(40) Kollmannsberger, M.; Rurack, K.; Resch-Genger, U.; Daub, J. *J. Phys. Chem. A* **1998**, *102* (50), 10211–10220.
(41) Qin, W.; Baruah, M.; Sliwa, M.; Van der Auweraer, M.; De Borggraeve, W. M.; Beljonne, D.; Van Averbeke, B.; Boens, N. *J. Phys. Chem. A* **2008**, *112* (27), 6104–6114.
(42) Klimant, I.; Huber, C.; Liebsch, G.; Neurauter, G.; Stangelmayer, A.; Wolfbeis, O. S. In *New Trends in Fluorescence Spectroscopy*; Valeur, P. B., Brochon, D. J.-C., Eds.; Springer Series on Fluorescence; Springer Berlin Heidelberg, 2001; pp 257–274.
(43) Accorsi, G.; Verri, G.; Bolognesi, M.; Armaroli, N.; Clementi, C.; Miliani, C.; Romani, A. *Chem. Commun.* **2009**, No. 23, 3392–3394.
(44) Harvey, H. W. *J. Mar. Biol. Assoc. U. K.* **1956**, *35* (1), 289–289.
(45) Millero, F. J.; Feistel, R.; Wright, D. G.; McDougall, T. J. *Deep Sea Res. Part Oceanogr. Res. Pap.* **2008**, *55* (1), 50–72.
(46) Caspers, H. *Int. Rev. Gesamten Hydrobiol. Hydrogr.* **1970**, *55* (1), 167–167.
(47) Müller, T. J. In *Methods of Seawater Analysis*; Grasshoff, K., Kremling, K., Ehrhardt, M., Eds.; Wiley-VCH Verlag GmbH, 1999; pp 41–73.
(48) Eilers, J. M.; Sullivan, T. J.; Hurley, K. C. *Hydrobiologia* **1990**, *199* (1), 1–6.
(49) Huber, C.; Klimant, I.; Krause, C.; Werner, T.; Mayr, T.; Wolfbeis, O. S. *Fresenius J. Anal. Chem.* **2000**, *368* (2–3), 196–202.

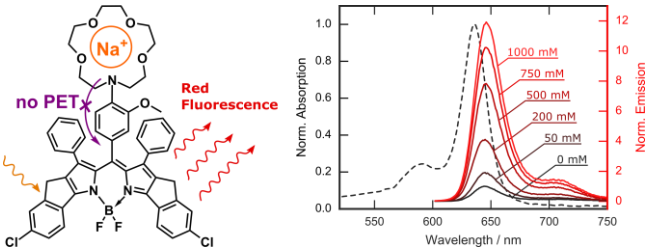
Na+
no PET
Red
Fluorescence
Cl
Cl
Norm. Absorption
Norm. Emission
Wavelength / nm
1000 mM
750 mM
500 mM
200 mM
50 mM
0 mM

For TOC only